Molecular Biology of the Cell
Vol. 19, 2339–2347, May 2008

Src-mediated Cortactin Phosphorylation Regulates Actin Localization and Injurious Blebbing in Acinar Cells

Vijay P. Singh and Mark A. McNiven

Department of Biochemistry and Molecular Biology and the Miles and Shirley Fiterman Center for Digestive Diseases, Mayo Clinic, Rochester, MN 55905

Submitted November 12, 2007; Revised February 8, 2008; Accepted March 3, 2008
Monitoring Editor: Josephine Adams

Suprastimulation of pancreatic acini is a well-known model for pancreatitis, and it is characterized by actin reorganization and cell blebbing. Currently, however, the mechanisms underlying regulation of these aberrant cytoskeletal and membrane dynamics and how they contribute to cell injury are unclear. We observed that suprastimulation results in a rapid activation of Src and relocalization of the actin-binding protein cortactin from the apical to the basolateral domain at the necks of membrane blebs. Furthermore, Src-mediated cortactin tyrosine phosphorylation was markedly increased after suprastimulation. Pretreatment of acini with Src inhibitors or expression of a cortactin tyrosine phospho-inhibitory mutant reduced actin redistribution and bleb formation induced by suprastimulation in vitro. Importantly, inhibition of Src activity in rat models of suprastimulation-induced pancreatitis substantially reduced disease severity, as indicated by a reduction in serum amylase and pancreatic edema and a striking improvement in tissue histology. These findings indicate a novel, disease-relevant role for Src-mediated cortactin phosphorylation in aberrant reorganization of the actin cytoskeleton, a mechanism that is likely to have implications in other types of cell injury. In addition, they suggest a potential use for Src inhibitors as an approach to reduce cell injury.

INTRODUCTION

Actin-mediated cortical blebbing plays an important role in both normal and pathological processes, ranging from apoptosis and necrotic cell death to cell migration and mitosis (Gourlay and Ayscough, 2005; Paluch *et al*., 2006). Suprastimulation (SS) of isolated pancreatic acini with high concentrations of secretagogue such as the G protein-coupled receptor agonist cholecystokinin (CCK) or the CCK analogue caerulein (CER) leads to a block in zymogen secretion that is accompanied by significant alterations in cell morphology and the actin cytoskeleton, including cell blebbing (Burnham and Williams, 1982; Adler *et al*., 1984; O'Konski and Pandol, 1990; Torgerson and McNiven, 1998). In addition, SS induces vacuole formation (Watanabe *et al*., 1984; Waterford *et al*., 2005), missorting and premature activation of nascent zymogens (Saito *et al*., 1987; Husain *et al*., 2005) as well as aberrant zymogen release from the basal membrane domain (Scheele *et al*., 1987). Indeed, SS results in cellular responses similar in many aspects to that observed in pancreatitis (Bhatia *et al*., 2005; Pandol *et al*., 2007), indicating its relevance as a disease model both in vitro and in animals (Lampel and Kern, 1977).

Along with actin, the actin-based motor protein myosin II undergoes a dramatic relocalization from the apical to the basolateral domain during SS of acini. Indeed, the activation of an actin–myosin network at the cell base seems to result in the formation of a contractile ring that mediates the protrusion of acinar cell blebs. In addition, these membranous extensions are extremely dynamic, forming within minutes of SS and undergoing cytoplasmic streaming as well as amoeboid-like movements. Importantly, cell blebs induced by SS do not seem to represent an apoptotic death response, because they can rapidly recede and reabsorb back into the cell upon removal of the insult (Torgerson and McNiven, 1998). Furthermore, the dramatic SS-induced changes in actin cytoskeletal organization in isolated acini seem to mimic those observed in the intact organ (Fallon *et al*., 1995; Jungermann *et al*., 1995). However, the mechanisms regulating changes in actin dynamics following SS are unclear as to whether reorganization of the actin cytoskeleton directly contributes to acinar cell injury or is simply a consequence of cell damage.

The actin-binding protein cortactin is a well-known component of the actin polymerization machinery in many cell types, and it is involved in the formation of branched actin networks that mediate membrane protrusion (Weed and Parsons, 2001; Weaver *et al*., 2003). In addition, cortactin is phosphorylated downstream of and regulates actin dynamics in response to various signaling pathways. Indeed, cortactin was identified as a major substrate of v-Src in transformed cells, and it is phosphorylated by various members of the Src family of nonreceptor tyrosine kinases (Daly, 2004; Lua and Low, 2005). The Src family kinase members c-Src, Yes, and Lyn have been reported to be expressed in pancreatic acinar cells as well as activated in response to SS (Nozu *et al*., 2000; Lynch *et al*., 2004; Pace *et al*., 2006). Therefore, we hypothesized that the aberrant actin reorganization and cell blebbing in response to SS could be a result of inappropriate activation of Src and subsequent increased cortactin tyrosine phosphorylation. Moreover, because Src inhibitory drugs

This article was published online ahead of print in *MBC in Press* (http://www.molbiolcell.org/cgi/doi/10.1091/mbc.E07–11–1130) on March 19, 2008.

Address correspondence to: Mark A. McNiven (mcniven.mark@mayo.edu).

Abbreviations used: CCK, cholecystokinin; CER, caerulein; M3 cortactin, a cortactin tyrosine phospho-mutant in which three key tyrosine residues have been mutated to phenylalanine; SS, suprastimulation; WT, wild type.

are commercially available, these could be used to test whether inhibition of Src activity in animal models of pancreatitis alleviates disease severity.

MATERIALS AND METHODS

Reagents

All experiments were approved by the Institutional Animal Care and Use Committee of the Mayo Clinic (Rochester, MN). Male (100–120 g) Sprague Dawley rats (Harlan, Indianapolis, IN) were housed and fed under standard conditions. Caerulein, a CCK analogue, was from Research Plus (Bayonne, NJ). Antibodies against phospho-tyrosine (4G10) and cortactin (4F11) were from Upstate Biotechnology (Charlottesville, VA). Anti-pan-Src (SC-18), anti-Fyn (SC-16), and anti-c-Src (H-12) antibodies were from Santa Cruz Biotechnology (Santa Cruz, CA). The antibody recognizing active Src family kinases, anti-phospho-Y416 (PY416), anti-Yes, and anti-Lyn antibodies were from BD Biosciences Transduction Laboratories (Lexington, KY). The polyclonal antibody against cortactin (AB3) was produced by our laboratory (Cao *et al.*, 2003). Secondary antibodies for immunofluorescence, conjugated to Alexa 488 or Alexa 594, and ProLong Gold were from Invitrogen (Carlsbad, CA). HRP-conjugated goat anti-rabbit and goat anti-mouse secondary antibodies for Western blotting were from Affinity BioReagents (Golden, CO). Collagenase type IV was from Worthington Biochemicals (Lakewood, NJ). PP2 and SU6656 were from Calbiochem (San Diego, CA), and they were dissolved in dimethyl sulfoxide (DMSO) as a 1000× stock. All other reagents were purchased from Sigma-Aldrich (St. Louis, MO).

Preparation and Use of Acini

Acini were harvested in the presence of 100 U/ml collagenase in a buffer containing 20 mM HEPES at pH 7.4, 120 mM NaCl, 5 mM KCl, 1 mM $MgCl_2$, 1 mM $CaCl_2$, 10 mM glucose, 10 mM sodium pyruvate, 0.1% bovine serum albumin, and 0.01% soybean trypsin inhibitor as described previously (Torgerson and McNiven, 1998). After isolation, acini were filtered through a 70-μm mesh (Fisher Scientific, Pittsburgh, PA), and they were kept at 37°C for 2 h before use. When indicated, acini were treated during the 2-h incubation with either 20 μM PP2 or 10 μM SU6656. Viability before use was >95%, as indicated by trypan blue exclusion. For experiments involving adenoviral-mediated infection, acini were cultured for 16 h in RPMI 1640 medium (Mediatech, Herndon, VA) with 10% fetal calf serum, 20 mM nicotinamide, 100 U/ml penicillin, and 100 μg/ml streptomycin (Invitrogen, Carlsbad, CA). Adenovirus was prepared by the University of Iowa Gene Transfer Vector Core by using the RAPAd system (U.S. Patent 6830,920B2, Anderson *et al.*, 2000). The cDNA sequence corresponding to rat cortactin isoform B (GenBank accession no. NM_021868) was used for generating the wild-type (WT) cortactin construct. The cortactin tyrosine phospho-mutant in which tyrosines 384, 429, and 445 were mutated to phenylalanines (M3 cortactin) was subsequently generated using the Stratagene QuikChange site-directed mutagenesis kit (Stratagene, La Jolla, CA). Virion encoding for WT cortactin or M3 cortactin were incubated with cells at 10^7 plaque-forming units/ml. To detect the expression of either WT cortactin or M3 cortactin, 16 h after infection, cells were processed for immunofluorescence or Western blot analysis by using the 4F11 or AB3 antibody, respectively.

Immunofluorescence Staining

Acini were plated on plain glass coverslips, fixed with 2% paraformaldehyde, and permeabilized with 0.6% Triton X-100 as described previously (Torgerson and McNiven, 1998). Acini were then blocked with 5% normal goat serum, incubated with primary antibodies (4F11, diluted 1:1000; SC-18, diluted 1:300; and anti-Yes, diluted 1:1000) for 1 h at room temperature, washed, and incubated with secondary antibodies (Alexa 488- or Alexa 594-conjugated, diluted 1:500) with or without rhodamine-conjugated phalloidin (100 nM; Invitrogen) for 30 min. After washing, acini were mounted in ProLong Gold (Invitrogen, Carlsbad, CA). Acini with six to 12 cells were randomly chosen and imaged using a Zeiss LSM510 confocal microscope (Thornwood, NJ). Images were processed using Adobe Photoshop 6.0 (Adobe Systems, Mountain View, CA). For quantitation of blebbing, the number of blebs was counted along with the number of cells. The result, reported as bleb number per 100 cells, represents the mean ± SEM for at least three independent experiments.

Immunoprecipitation and Western Blot Analysis

Acini or tissue were homogenized in a buffer containing 50 mM Tris at pH 7.2, 150 mM NaCl, 0.5 mM EDTA, 1 mM EGTA, 2 mM dithiothreitol, 1 mM Na_3VO_4, 25 mM NaF, 1% NP-40, and Complete (Roche Diagnsotics, Indianapolis, IN) protease inhibitor cocktail. Lysates were either boiled in 1× Laemmli sample buffer before Western blot analysis according to standard procedures or used for immunoprecipitation. In this case, lysates were incubated with 5 μg/ml primary antibody for 2 h at 4°C, followed by addition of 4 mg of protein A beads for 1 h in the same buffer. The beads were then washed three times, boiled in 1× Laemmli sample buffer, and analyzed by Western blot. The following antibodies were used at the indicated dilutions for Western blot analyses: AB3 (1:1,000,000), 4G10 (1:1000), SC-18 (1:500), anti-PY416 (1:1000), anti-Yes (1:5000), H-12 (1:200), anti-Fyn (1:200), and anti-Lyn (1:200). Band intensity was quantified by densitometry using the Bio-Rad Image Analysis System with Molecular Analyst software and a Bio-Rad Model GS-700 imaging densitometer (Bio-Rad, Hercules, CA). The levels of phosphorylated protein were normalized to total levels of the respective protein. For coimmunoprecipitation experiments, the levels of coimmunoprecipitated protein were normalized to the levels of the primary immunoprecipitated protein, i.e., the protein against which the antibody used for immunoprecipitation was made. The reported results are based on quantitation performed using at least two independent experiments for each assay.

Blood and Tissue Preparation

Animals (6 animals in each group) were given single intraperitoneal injections of saline (control) or 20 μg/kg caerulein in saline by using standard procedures. Blood and tissue samples were harvested 6 h later, and either frozen or fixed in 4% formaldehyde. When used, PP2 was dissolved in DMSO and injected intraperitoneally (3 mg/kg in 0.1 ml) 30 min before caerulein. Animals pretreated with vehicle were given DMSO only.

Morphological Examination and Assays

Five-micrometer sections of paraffin-embedded pancreas were stained with hematoxylin and eosin (H&E). For immunohistochemistry of pancreas, 5-μm sections of tissue embedded in Optimal Cutting Temperature compound (Tissue-Tek, Sakura Finetek, Torrance, CA) were fixed with 4% paraformaldehyde and immunostained as described above. Serum amylase activity was measured colorimetrically using the Phadebas assay (Pharmacia Diagnostics, Portage, MI). Edema was measured by subtracting the dry weight from the wet weight, and the data are reported as a percentage of wet weight.

Statistical Analyses

The results reported represent the mean ± SEM of values obtained from three or more experiments, and they were compared using the Student's *t* test when the data consisted of only two groups or analysis of variance (ANOVA) when comparing three or more groups. If ANOVA indicated a significant difference, the data were analyzed using Tukey's method as a post hoc test for the difference between groups. A p value of 0.05 was considered significant.

RESULTS

Suprastimulation of Pancreatic Acini Leads to Src-mediated Cortactin Phosphorylation along with Reorganization of the Actin Cytoskeleton

Under resting conditions or after stimulation of pancreatic acini with physiological concentrations of CCK (<0.1 nM), a rich network of filamentous actin is present at the apical membrane domain (Figure 1aa′), a partial disassembly of which supports the proper secretion of zymogens into the lumen (Muallem *et al.*, 1995). In contrast, stimulation with supraphysiologic concentrations of CCK (10 nM) induces a marked redistribution of actin from the apical to the basolateral domain where it seems to support the formation of large, dynamic blebs (Figure 1a″; Burnham and Williams, 1982; Adler *et al.*, 1984; O'Konski and Pandol, 1990; Torgerson and McNiven, 1998). Interestingly, we observed that the actin-binding protein cortactin is also localized apically after stimulation with physiological concentrations of CCK (Figure 1b′) and that it becomes redistributed in a manner similar to that of actin after SS (Figure 1b″).

The actin-binding and -regulatory properties of cortactin are modulated in response to tyrosine phosphorylation by nonreceptor tyrosine kinases such as Src family kinases (Weed and Parsons, 2001; Daly, 2004; Lua and Low, 2005). Therefore, we tested whether SS leads to tyrosine phosphorylation of cortactin and might thus accompany actin and cortactin redistribution. Here, pancreatic acini were isolated from rats, treated with various concentrations of CCK for 2 min, a time frame in which bleb formation occurs in the presence of SS, lysed, and subjected to immunoprecipitation by using antibodies against cortactin. Subsequently, the immunoprecipitated samples were analyzed by Western blot for tyrosine phosphorylated cortactin by using anti-cortactin and anti-phospho-tyrosine (4G10) antibodies. Indeed, sup-

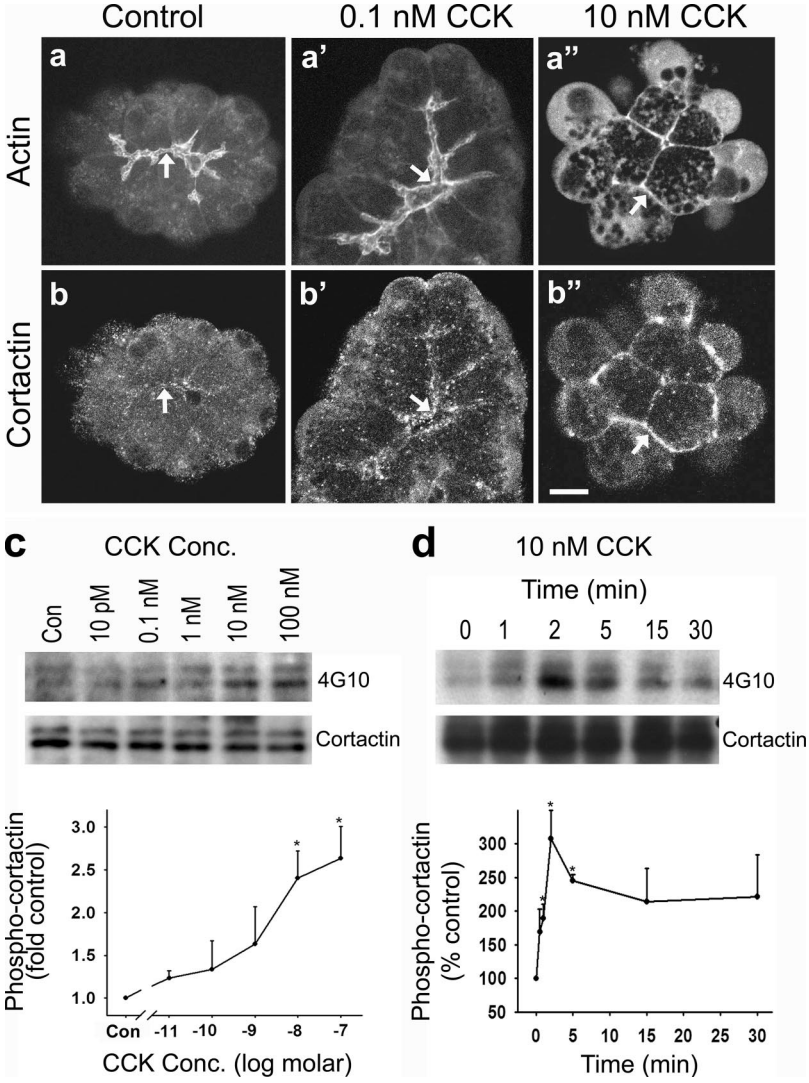

Figure 1. Cortactin is tyrosine phosphorylated upon SS of pancreatic acini and relocalizes to the necks of basolateral blebs. (a–b″) Fluorescence micrographs of actin and cortactin in resting acini (Control) and in acini treated with physiological (0.1 nM) or supraphysiological (10 nM) concentrations of CCK. In resting cells, a rich apical network of actin surrounds the lumen (a, arrow); however, only a modest amount of cortactin localizes to this region (b, arrow). Actin remains apical after stimulation with 0.1 nM CCK (a′, arrow), whereas the apical localization of cortactin is enhanced (b′, arrow). In contrast, SS with 10 nM CCK induces blebbing and a marked redistribution of both actin (a″) and cortactin (b″) to the necks of basal blebs (arrows). Bar, 10 μm (a–b″). (c) Cortactin tyrosine phosphorylation increases after SS with CCK. Acini were left untreated (Con) or stimulated with logarithmically increasing doses of CCK (10 pM–100 nM) for 2 min before immunoprecipitation of lysates by using an antibody against cortactin. The samples were subsequently analyzed by Western blot using an anti-phospho-tyrosine antibody (4G10), and band intensity was quantified by densitometry. As depicted in the graph, cortactin tyrosine phosphorylation was increased significantly (2- to 3-fold) at doses of 10 nM CCK or higher (i.e., SS). (d) Tyrosine phosphorylation of cortactin occurs rapidly in response to SS. Lysates from acini were analyzed as described in c; however, in response to a single dose of 10 nM CCK at the indicated time points of 0–30 min. A marked increase in cortactin tyrosine phosphorylation was observed within 2 min of SS, and it remained elevated over the 30-min time course. Graphs represent the mean ± SEM from at least two independent experiments. *p ≤ 0.05.

raphysiological concentrations of CCK stimulated a two- to threefold increase in cortactin tyrosine phosphorylation compared with basal conditions or stimulation with physiological CCK concentrations (Figure 1c). A more detailed analysis of SS-induced cortactin tyrosine phosphorylation indicated that this phosphorylation was rapid, peaking around 2 min, and that it was sustained for >30 min (Figure 1d).

Different Src family kinases (c-Src, Yes, and Lyn) have been found to be activated in response to SS of pancreatic acini (Nozu *et al*., 2000; Lynch *et al*., 2004; Pace *et al*., 2006); therefore, they might mediate cortactin tyrosine phosphorylation. Thus, we first used immunofluorescence analysis to determine the localization of Src (anti-pan-Src antibody) with respect to cortactin in isolated acini under basal conditions and after stimulation with different concentrations of CCK. Resting cells displayed a marked colocalization between Src and cortactin at the apical membrane domain adjacent to the lumen, which extended down along the lateral membrane domains (Figure 2aa′). This codistribution of Src and cortactin was maintained after stimulation of acini with physiological concentrations of CCK (0.1 nM) over 30 min (Figure 2ee′). Interestingly, after just 5 min of SS (10 nM CCK), both Src and cortactin translocated away from the apical lumen (Figure 2bb′), and by 30 min Src they seemed to become largely cytosolic, whereas cortactin accumulated along the necks of newly protruding blebs (Figure 2cc′). Importantly, this dramatic dissociation and redistribution of Src and cortactin was prevented in acini treated with the Src inhibitory drug PP2 (20 μM) for 2 h before SS (Figure 2dd′), supporting that Src-mediated phosphorylation of cortactin leads to its redistribution.

As an extension of the morphological observations, we next used a biochemical approach to analyze the association between Src and cortactin under different conditions of CCK stimulation. Pancreatic acini were isolated, treated with different concentrations of CCK for 2 min, and then subjected to immunoprecipitation by using an anti-pan-Src antibody. The immunoprecipitated samples were then analyzed by Western blot using antibodies against Src and cortactin. Under resting conditions or in acini treated with low concentrations of CCK (10 pM), substantial levels of cortactin coimmunoprecipitated along with Src (Figure 2f). However, the Src–cortactin complex seemed to dissociate in a CCK concentration-dependent manner, with essentially no complex being detected in acini treated with CCK concentrations representing SS. Importantly, dissociation of the Src–cortactin complex after SS was prevented by pretreating acini with

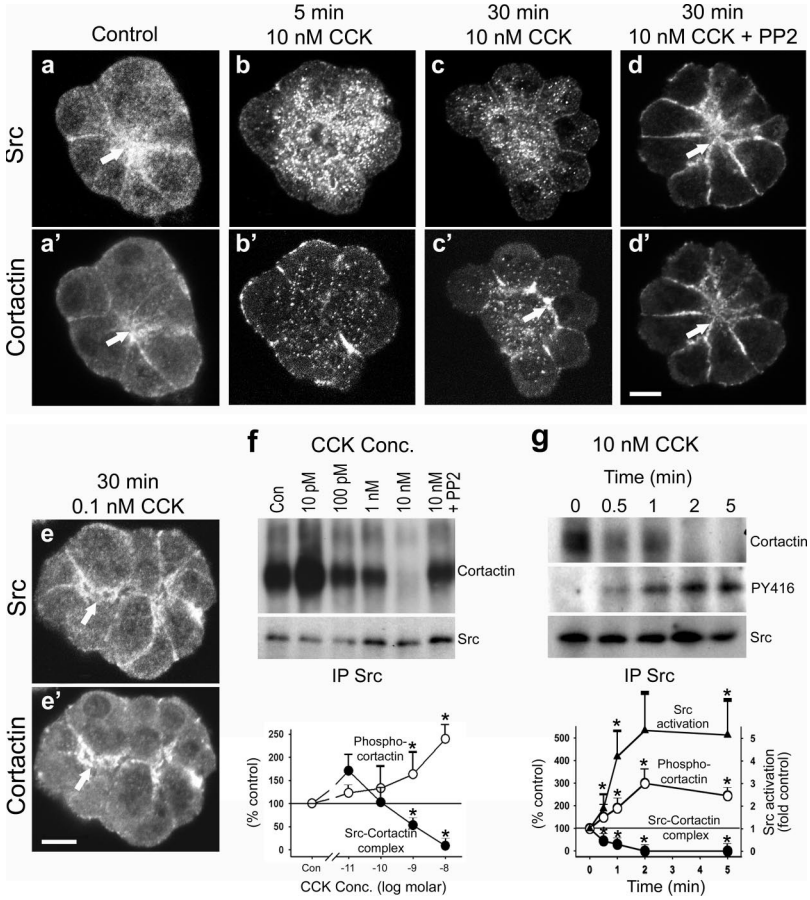

Figure 2. SS induces Src-mediated cortactin phosphorylation and dissociation of a Src-cortactin complex. (a–e′) Fluorescence micrographs of acini stained for Src and cortactin. Under resting conditions (Control; a and a′) or after stimulation with physiological CCK concentrations (0.1 nM CCK; e and e′), Src and cortactin colocalize at the apical region of acini (arrows). However, SS of acini (10 nM CCK) induces a relocalization of cortactin to the basolateral membrane domain within 5 min (b′), which becomes more pronounced at 30 min as the acini bleb (c′, arrow). Src, in contrast, becomes cytosolic after SS (b and c). Treatment of acini with the Src family kinase inhibitor PP2 before SS prevents the redistribution of cortactin and Src, because they both remain apical (d and d′, arrows). Bars, 10 μm (a–e′). (f) A Src–cortactin complex, present at low concentrations of CCK, dissociates after SS. Lysates from resting acini (Con) or acini stimulated with increasing doses of CCK (10 pM–10 nM) or with 10 nM CCK + PP2 were subjected to immunoprecipitation by using an anti-pan-Src antibody, and the samples were analyzed by Western blot using antibodies against cortactin and Src. Band intensity was quantified by densitometry, normalizing the cortactin levels to the Src levels. As indicated by the graph, the Src–cortactin complex dissociates in a dose-dependent manner with little, if any, complex being detected after SS. Pretreatment with PP2, however, prevents this dissociation. (g) Dissociation of the Src–cortactin complex is rapid, and it correlates with cortactin tyrosine phosphorylation. Lysates from acini stimulated with 10 nM CCK for the indicated amounts of time (0–5 min) were immunoprecipitated for Src and analyzed by Western blot, using antibodies against cortactin, Src, and activated Src (PY416). Band intensity was quantified by densitometry, normalizing the cortactin and activated Src levels to total Src levels. The Src–cortactin complex dissociates rapidly, within 1 min after SS. In addition, this dissociation correlates with increased cortactin phosphorylation (see Figure 1D) and Src activation (graph). Graphs represent the mean ± SEM.

PP2, thus inhibiting Src activity (Figure 2f). Indeed, we observed a strong inverse correlation between the levels of tyrosine phosphorylated cortactin and the detection of a Src–cortactin complex over increasing concentrations of CCK (Figure 2f, graph). Further analysis of the SS-induced dissociation of the Src–cortactin complex over a time course of 5 min indicated a rapid disassembly of the complex (<2 min) that correlated with Src activation, as determined by Western blot analysis of the immunoprecipitated samples with an antibody against a phospho-active form of Src (phospho-Y416, PY416; Figure 2g). Thus, these morphological and biochemical observations suggest that a Src–cortactin complex is present under resting and physiological stimulatory conditions. However, SS induces Src activation, leading to increased cortactin tyrosine phosphorylation, dissociation of the complex, and a differential redistribution of these proteins as well as the actin cytoskeleton.

Activation of Src Induces Acinar Cell Damage after Suprastimulation

As indicated above, several Src family members are expressed in pancreatic acinar cells, and they become activated in response to SS (Nozu *et al*., 2000; Lynch *et al*., 2004; Pace *et al*., 2006). The above-mentioned studies were performed using an anti-pan-Src antibody, which recognizes multiple Src kinase family members. Therefore, to discern the specific Src family member associated with cortactin, lysates from pancreatic acini were subjected to immunoprecipitation by using either the anti-pan-Src or an anti-cortactin antibody, and the samples were analyzed by Western blot for c-Src, Yes, Lyn, and Fyn. Interestingly, although all four Src family members were detected in whole cell lysates, only Yes was immunoprecipitated by the anti-pan-Src antibody; furthermore, Yes coimmunoprecipitated with cortactin (Supplemental Figure S1, a and b). Subsequent analysis of lysates from resting and CCK-stimulated (10 pM–10 nM) acini immunoprecipitated for Yes indicated that Yes is activated after SS, as determined by using the anti-PY416 antibody (Supplemental Figure S1c; Lynch *et al*., 2004). Finally, immunofluorescence analysis of resting acini and acini stimulated with either physiological (0.1 nM) or supraphysiological (10 nM) concentrations of CCK for 30 min supported that Yes and cortactin colocalize under physiological conditions (Supplemental Figure S1, d and e′), whereas they become redistributed after SS (Supplemental Figure S1, f and f′). Importantly, this relocalization of Yes and cortactin was prevented in acini treated with PP2 before SS (Supplemental Figure S1, g and g′). These results suggest that Yes associates with cortactin under physiological conditions and mediates cortactin tyrosine phosphorylation after SS; however, we cannot rule out a role for other Src family members. Thus, the term "Src" is used from here on with the intended meaning of Yes as well as potentially other Src kinases.

Pharmacological inhibition of Src activity with PP2, a small-molecule inhibitor of multiple Src family kinases, as well as SU6656 (data not shown; see below), another Src

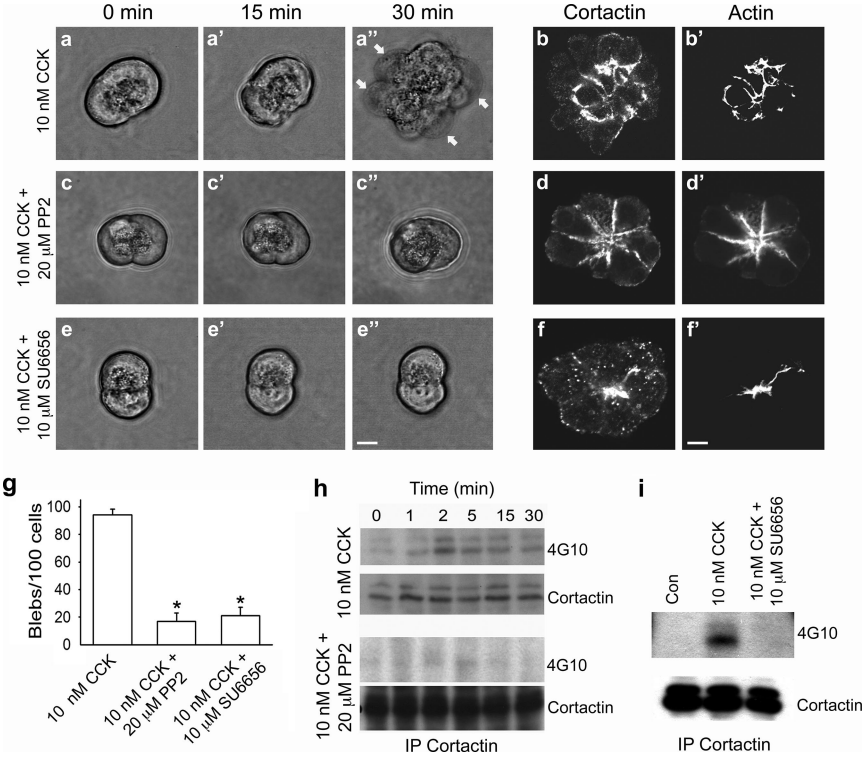

Figure 3. Inhibition of Src reduces SS-induced cortactin tyrosine phosphorylation, cortactin and actin redistribution, and bleb formation. (a–f′) Micrographs of living and fixed acini after SS with 10 nM CCK in the absence or presence of either 20 μM PP2 or 10 μM SU6656. Living acini were observed to form blebs over a 30-min time course of SS with CCK (a–a″, arrows). Under similar conditions, immunofluorescence analysis of fixed acini showed a redistribution of cortactin and actin to the necks of basolateral blebs (b and b′). However, treatment of acini with either of the Src inhibitory drugs PP2 or SU6656 before and during SS resulted in a significant reduction in bleb formation in living acini (c–c″ and e–e″, respectively) as well as prevented cortactin and actin redistribution, as indicated by subsequent immunofluorescence analysis of fixed acini (d and d′ and f and f′). Bars, 10 μm (a–f′). (g) Quantitation of SS-induced acinar blebbing in the absence and presence of either PP2 or SU6656 revealed a substantial reduction (>75%) in bleb formation in drug-treated acini (150–300 cells were counted for each treatment). (h and i) Treatment with Src family kinase inhibitors reduces cortactin tyrosine phosphorylation after SS. Lysates from unstimulated acini (0 min, h; Con, i) or acini stimulated with 10 nM CCK alone or in the presence of either PP2 (h) or SU6656 (i) were immunoprecipitated for cortactin and analyzed by Western blot using antibodies against cortactin and phospho-tyrosine (4G10).

family kinase inhibitory drug, prevented the dissociation of the Src–cortactin complex as well as redistribution of cortactin to the necks of basal membrane blebs normally observed after SS (Figures 1 and 2, and Supplemental Figure S1). Therefore, we next tested whether treatment of acini with either of these Src inhibitors might inhibit acinar cell blebbing. Living and fixed acini were imaged after SS with 10 nM CCK both in the presence and absence of treatment with Src inhibitors (PP2, 20 μM; SU6656, 10 μM), and bleb formation was quantified (Figure 3, a–g). In the absence of Src inhibitors, acini were observed to undergo significant blebbing within 30 min of SS (Figure 3, a–a″). In addition, imaging of fixed acini treated in a similar manner and stained for cortactin and actin indicated a relocalization of these proteins to the necks of membrane blebs, as expected (Figure 3, bb′). In striking contrast, acini treated with either PP2 (Figure 3, c–c″) or SU6656 (Figure 3, e–e″) before and during SS with CCK maintained a near normal shape over the 30-min time period. Accordingly, immunofluorescence analysis of Src inhibitor-treated acini revealed that the apical localization of cortactin and actin was maintained (Figure 3d, d′, f, and f′). Quantitation of >100 acinar cells indicated a significant reduction (>75%) in blebbing in cells treated with either of the Src inhibitory drugs in combination with SS compared with cells treated with supraphysiological concentrations of CCK alone (Figure 3g). Importantly, Western blot analysis of acini treated with 10 nM CCK (i.e., SS) in the presence or absence of either PP2 (Figure 3h) or SU6656 (Figure 3i) by using the anti-phospho-tyrosine antibody 4G10 indicated that both drugs inhibited cortactin tyrosine phosphorylation. Thus, Src-mediated phosphorylation of cortactin seems to regulate cell blebbing in response to SS of pancreatic acinar cells. Importantly, PP2 did not affect the secretory response of acini (amylase activity) under control conditions (5.6 + 2.3 vs. 6.0 + 2.5%), or in response to physiological (0.1 nM; 18.4 + 1.8% vs. 18.0 + 2.3%) or supraphysiological (10 nM; 11.0 + 1.9% vs. 11.0 + 2.5%) concentrations of CCK.

The reduction in acinar cell blebbing upon inhibition of Src family kinases could be a result of effects on proteins in addition to cortactin. Therefore, we next tested whether tyrosine phosphorylation of cortactin plays a direct role in SS-induced acinar cell damage. Toward this end, a tyrosine phospho-mutant of cortactin was constructed in which three tyrosine residues shown previously to be predominant sites of Src-mediated phosphorylation (Huang *et al.*, 1998) were mutated to phenylalanine and expressed in cultured acini after adenovirus-mediated infection. Subsequently, the effects of this phospho-mutant protein, referred to as M3 cortactin, on cortactin localization and cell blebbing in response to SS were analyzed. Remarkably, acini expressing M3 cortactin maintained an apical cortactin and actin localization after SS; more importantly, they did not undergo cell blebbing (Figure 4, a–a″), which was in marked contrast to adjacent uninfected acini or acini infected with WT cortactin (data not shown). In support of these observations, quantitation of >100 acinar cells indicated a >50% reduction in SS-induced cell blebbing in cells expressing M3 cortactin compared with uninfected control cells or cells expressing WT cortactin (Figure 4b).

We observed that Src-mediated phosphorylation of cortactin after SS results in a dissociation of the endogenous Src–cortactin complex and a redistribution of these proteins. Therefore, we tested whether tyrosine phosphorylation of M3 cortactin was indeed reduced, and additionally, whether the Src–M3 cortactin complex was maintained in response to SS. Western blot analysis to quantitate the levels of adenoviral overexpression of WT and M3 cortactin showed a 14.5- and 10.3-fold overexpression over controls (data not shown). Furthermore, acini expressing WT or M3 cortactin revealed

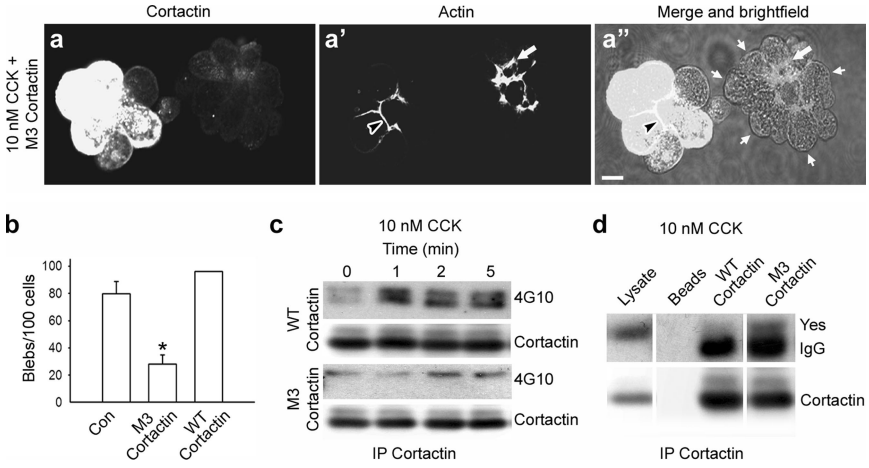

Figure 4. Expression of a cortactin tyrosine phospho-mutant significantly attenuates SS-induced acinar blebbing. (a–a″) Fluorescence and merged fluorescence + brightfield micrographs of an uninfected acinus (right) and an acinus expressing a cortactin mutant in which three key tyrosine residues have been mutated to phenylalanine (M3 cortactin, left). After 30 min of SS, cells were stained for cortactin (a) and actin (a′). In uninfected cells, actin relocalized to the basolateral membrane domain (a′ and a″, white arrows) and cells formed large blebs (a″, small white arrows). In contrast, cells expressing M3 cortactin retained an apical actin network (a′ and a″, black arrowheads), and they did not form blebs. Bar, 10 μm (a–a″). (b) Graph depicting the reduction in SS-induced bleb formation in cells expressing the cortactin tyrosine phospho-mutant, M3 cortactin (>50%), compared with uninfected control cells (Con) or cells expressing WT cortactin. Results represent the mean ± SEM from at least three independent experiments. (c) SS-induced tyrosine phosphorylation of cortactin is reduced in cells expressing the M3 cortactin mutant. Acini infected to express WT cortactin or M3 cortactin were stimulated with 10 nM CCK for the indicated amounts of time (0–5 min), lysed, and subjected to immunoprecipitation for cortactin followed by Western blot analysis using antibodies against cortactin and phospho-tyrosine (4G10). (d) The Src family kinase Yes coimmunoprecipitates with M3 cortactin, but not WT cortactin, following SS. Cortactin was immunoprecipitated from acini expressing WT cortactin or M3 cortactin after 1 min of SS. The immunoprecipitated samples as well as whole cell lysate and nonspecific proteins bound to beads alone were analyzed by Western blot using an anti-Yes antibody. The IgG band, which is detected just below the Yes band, is indicated. *$p \leq 0.05$ (b).

a reduction in phospho-tyrosine levels of M3 cortactin after SS (1.25-fold at 2 min), and, accordingly, an increased association with Src compared with WT cortactin (2.85-fold at 2 min) (Figure 4cd). Together, these results support a direct role for cortactin tyrosine phosphorylation in SS-induced acinar cell blebbing and injury.

Inhibition of Src Family Kinases Mitigates Disease Severity in the Caerulein Rat Model of Pancreatitis

Stimulation of isolated pancreatic acini or infusion of animals with supraphysiological concentrations of secretagogue represent models for studying pancreatitis (Bhatia *et al*., 2005; Pandol *et al*., 2007). Thus, we next tested whether our in vitro results might translate to the intact pancreas in an animal model of pancreatitis. For these studies, we first analyzed Src activation and cortactin phosphorylation over a 30-min time course by using lysates of pancreata harvested from individual rats for each time point after intraperitoneal injection of the CCK analogue CER (20 μg/kg). Similar to our in vitro results (Figure 2g), there was a rapid 2.2-fold activation of Src within 1 min of in vivo SS, and this was sustained over 30 min (Figure 5ac). In addition, Western blot analysis using the anti-phospho-tyrosine antibody 4G10 after immunoprecipitation of cortactin indicated that cortactin tyrosine phosphorylation was increased within 5 min and that it was even more prominent at 30 min (Figure 5b). Remarkably, intraperitoneal administration of 3 mg/kg PP2 30 min before a 30-min stimulation with CER inhibited the SS-induced increase in cortactin tyrosine phosphorylation (Figure 5d). In agreement with these biochemical results, morphological analysis of pancreas sections from control rats and rats treated with CER for 30 min in the presence or absence of PP2 showed that PP2 treatment prevented the CER-induced relocalization of actin and cortactin from the apical to the basolateral domain in vivo (Figure 5, e–g′). Thus, in isolated acini as well as the intact pancreas, inhibition of Src family kinases attenuates Src activation, cortactin tyrosine phosphorylation, and actin and cortactin redistribution in response to SS.

We next tested in more detail whether PP2 treatment might protect against SS-induced pancreatitis by using three main criteria: serum amylase levels, pancreatic edema, and tissue histology (Bhatia *et al*., 2005; Pandol *et al*., 2007). For these experiments, control animals and rats exposed to 20 μg/kg CER for 6 h in the presence or absence of PP2 were analyzed. An increase in serum amylase levels can be used as an indicator of loss of acinar cell polarity and subsequent cell death, resulting in aberrant release of zymogens into the blood space. In addition, as aberrant zymogen release, cell death, and inflammation increase, the pancreas becomes edematous. Indeed, treatment of rats with high concentrations of CER increased both of these parameters compared with control animals. Importantly, prophylactic treatment of rats with 3 mg/kg PP2 before CER administration markedly reduced the CER-induced aberrant release of amylase (>50% reduction) as well as increase in edema (Figure 6ab). However, most impressive was the morphological improvement of acinar structure as assessed by histology. Sections of normal pancreas displayed a polarized, well-organized arrangement of acini with zymogen granules clustered at the apical lumen (Figure 6c). In contrast, SS with CER resulted in the formation of large intracellular vacuoles and extensive interstitial edema and inflammation (Figure 6d). Remarkably, the pancreata from rats pretreated with PP2 seemed undamaged, with well-organized acini that mimicked control tissue (Figure 6e). To test for an effect of the src inhibitors on inflammatory cell infiltration, we quantified the number of white blood cells observed in 25 high power fields (HPF) of each variable of pancreatic sections from CER-treated mice pretreated with either PP2 or vehicle. We observed a reduction of white cells in pancreatic tissue from the PP2-treated animals (17.0 + 2.0 HPF in the caerulein pancreatitis group to 4.9 + 1.1 [$p < 0.005$] in the PP2-pretreated group). Vehicle had no effect on this (19.6 + 3.7 inflammatory cells/HPF; $p = 0.53$). This observation suggests that the inhibition of *src* activity could also exert some positive protective effects on the pancreas by reducing acinar-based blebbing and inflammation as well.

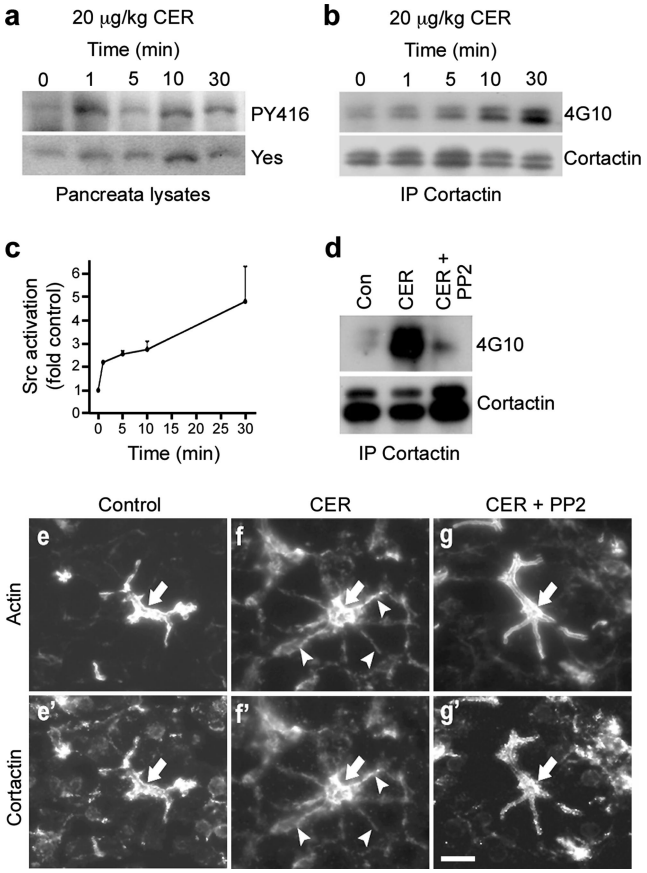

Figure 5. Src-mediated cortactin phosphorylation as well as relocalization of cortactin and actin occurs during CER-induced pancreatitis in vivo. (a–c) Src (Yes) is activated and cortactin is tyrosine phosphorylated in rats treated with supraphysiological concentrations of the CCK analogue CER, thus mimicking acute pancreatitis. Lysates were prepared from pancreata of animals after different times (1–30 min) of CER administration (20 μg/kg) via intraperitoneal injection. Lysates from pancreata of untreated animals were used as a control (Con). Whole cell lysates were analyzed by Western blot using an anti-Yes antibody and an antibody that recognizes the activated form of Src family kinases (PY416) (a). In addition, lysates were subjected to immunoprecipitation for cortactin, and the resulting samples were analyzed by Western blot for cortactin and phospho-tyrosine (4G10) (b). Bands representing Yes activation (PY416 signal) were quantified using densitometry, normalizing to total levels of Yes (c; n = 3). (d) PP2 treatment of intact pancreas reduces cortactin tyrosine phosphorylation. Lysates prepared from pancreata of untreated animals (Con), animals treated with 20 μg/kg CER for 30 min alone (CER), or animals treated with 3 mg/kg PP2 for 30 min before injection with 20 μg/kg CER for 30 min (CER + PP2) were immunoprecipitated for cortactin and analyzed by Western blot using antibodies against cortactin and phospho-tyrosine (4G10). (e–g′) Inhibition of Src activity by PP2 prevents CER-induced actin and cortactin relocalization in vivo. Fluorescence micrographs of frozen sections of rat pancreas from animals treated as described in d, and they were stained for actin (e, f, and g) and cortactin (e′, f′, and g′). A prominent apical localization of actin and cortactin is observed in pancreas sections from control animals (e and e′, arrows); however, they undergo a basolateral relocalization in response to SS with CER (f and f′, arrows). Remarkably, pretreatment with PP2 prevents this redistribution (g and g′, arrows). Bar, 10 μm (e–g′).

DISCUSSION

Many studies using experimental models of acute pancreatitis have focused on the consequences of SS of either

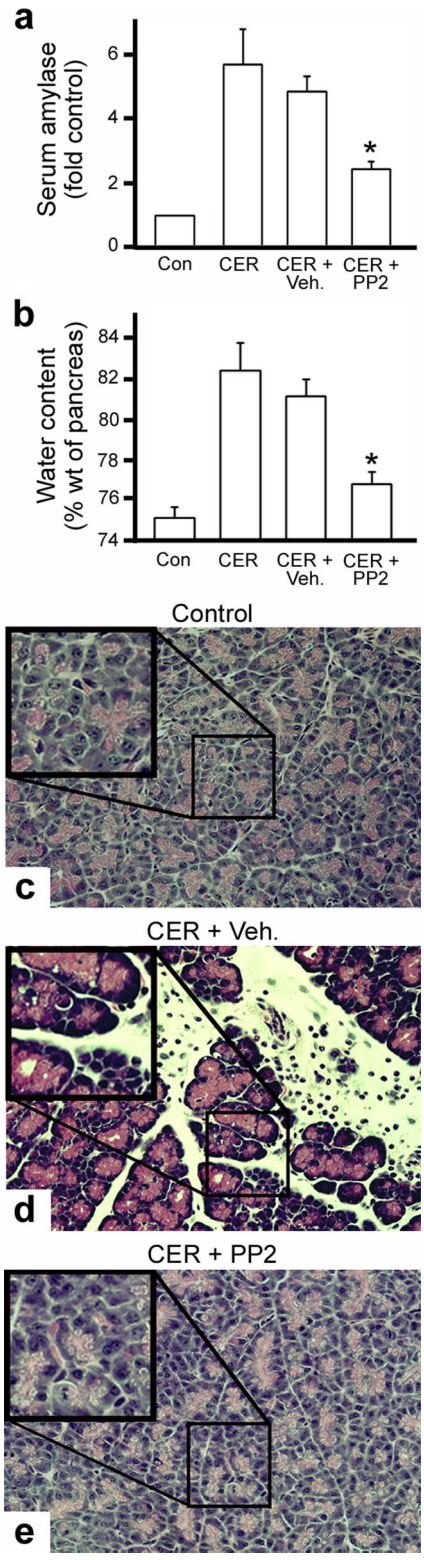

Figure 6. Inhibition of Src family kinases significantly reduces the severity of CER-induced pancreatitis in the intact animal. (a and b) Treatment of intact animals with PP2 reduces the CER-induced increase in serum amylase levels and pancreatic edema. Serum amylase (a) and pancreatic water content (b) were measured for untreated animals (Con), or those given a single intraperitoneal injection of 20 μg/kg CER, CER with vehicle (CER + Veh.), or 3 mg/kg PP2 dissolved in 0.1 ml of DMSO 30 min before CER injection and killed 6 h after the CER injection (CER + PP2). (c–e)

isolated pancreatic acini or animals with different agonists. It is well documented that a dramatic reorganization of the actin cytoskeleton is induced by these conditions both in vitro and in vivo (Burnham and Williams, 1982; Adler *et al*., 1984; O'Konski and Pandol, 1990, 1993; Fallon *et al*., 1995; Jungermann *et al*., 1995; Torgerson and McNiven, 1998). The mechanisms regulating this aberrant redistribution are unclear; moreover, it has yet to be determined whether this alteration in actin cytoskeletal organization plays a causal role in acinar cell injury or whether it is simply a result of cell damage. Here, we report an essential role for Src-regulated actin reorganization during acinar cell injury. Furthermore, we demonstrate that the actin-binding protein cortactin, a known Src substrate, mediates this aberrant reorganization of the actin cytoskeleton in a tyrosine phosphorylation-dependent manner. Importantly, inhibition of Src family kinases using either of the small-molecule inhibitors PP2 or SU6656 reduced acinar cell damage both in vitro and in the caerulein rat model of pancreatitis, indicating the potential usefulness of Src inhibitory drugs in the therapeutic treatment of pancreatitis.

Src family kinases, including Yes, have previously been found to be activated after SS of isolated acini (Nozu *et al*., 2000; Lynch *et al*., 2004; Pace *et al*., 2006), and they are implicated indirectly in disassembly of the actin cytoskeleton (Leser *et al*., 2000; Lynch *et al*., 2004). Here, we demonstrate a direct role for a SS-induced increase in tyrosine phosphorylation of cortactin by a Src family kinase, most likely Yes, in relocalization of the actin cytoskeleton and acinar cell damage. Treatment of isolated acini with Src inhibitors (PP2 or SU6656) before SS prevented the aberrant redistribution of the actin cytoskeleton and cell blebbing (Figure 3), suggesting that Src activation and subsequent actin reorganization play a causal role in cell damage. However, various downstream Src substrates such as the focal adhesion protein Pyk2 (Lynch *et al*., 2004), the cell–cell junction protein p120 catenin (Leser *et al*., 2000) as well as others might be responsible for mediating the altered actin organization and cell damage. Our observation that expression of a cortactin tyrosine phospho-mutant (M3 cortactin) prevents disassembly of the apical network of filamentous actin, while also leading to a significant reduction in cell blebbing after SS (Figure 4), provides a direct link between Src activation and aberrant actin reorganization during acinar cell injury. Most importantly, these findings support the concept that changes in actin cytoskeletal organization are a primary event in acinar cell damage. In essence, no cortactin tyrosine phosphorylation, no aberrant SS-induced actin rearrangement, no cell damage.

In addition to our observations in isolated acini, these findings translated to the caerulein rat model of pancreatitis. Activation of Yes and cortactin tyrosine phosphorylation were rapidly increased in the intact pancreas of stimulated animals; moreover, cortactin and actin underwent a dramatic basolateral redistribution (Figure 5). Importantly, these effects as well as overall disease severity, as indicated by a decrease in serum amylase levels and pancreatic edema, and most remarkably, restoration of tissue integrity to near that of control animals, were alleviated by treatment of animals with the Src inhibitor PP2 before CER administration (Figures 5 and 6). Thus, these results provide an exciting and necessary extension of previous studies implicating Src family kinases in pancreatic acinar cell injury, while highlighting the in vivo relevance of aberrant Src-mediated cortactin phosphorylation and subsequent actin reorganization in cell damage during pancreatitis.

The formation of basolateral cell blebs in isolated acini after SS is thought to be mediated by activation of an actin–myosin contractile network at the cell base (Burnham and Williams, 1982; Adler *et al*., 1984; O'Konski and Pandol, 1990; Torgerson and McNiven, 1998). Because inhibition of Src activation and cortactin phosphorylation prevented cell blebbing (Figures 3 and 4), potentially the improper Src-induced, cortactin-mediated assembly of actin at the acinar cell base provides a means for actin–myosin contraction at a site in which it is not needed or preferred. We (Torgerson and McNiven, 1998) and others (Burnham *et al*., 1988) have observed an increase in phosphorylated myosin light chain after SS of acini, and this correlates with activation of myosin II at the necks of cell blebs (Torgerson and McNiven, 1998). Interestingly, tyrosine phosphorylated cortactin has been demonstrated to bind myosin light chain kinase from endothelial cells and increase its activity, as indicated by increased myosin light chain phosphorylation (Garcia *et al*., 1999; Dudek *et al*., 2004). Similar to actin and myosin II, we observed that cortactin is redistributed to the necks of cell blebs after SS (Figures 1 and 3). Thus, SS-induced tyrosine phosphorylation of cortactin by Yes may mediate redistribution as well as activation of the actin–myosin contractile network, thereby directly contributing to acinar cell blebbing and injury.

Cortactin is involved in a variety of cellular processes, including migration, adhesion, and vesicle trafficking. In addition, phosphorylation plays an important role in regulating the effects of cortactin on actin dynamics and cytoskeletal organization (Weed and Parsons, 2001; Daly, 2004; Lua and Low, 2005). Thus, the increase in cortactin phosphorylation after SS could lead to undesirable changes in cell–cell contacts, actin–myosin contractility, and/or membrane protrusion, thereby contributing to bleb formation and cell damage. The findings reported here emphasize the importance of understanding how actin dynamics are regulated in pancreatic acinar cells, while providing significant insight into the molecular basis of acinar cell injury. Most excitingly, these results highlight Src as an attractive therapeutic target for the treatment of acute pancreatitis, a disease for which no treatment currently exists.

Figure 6 (cont). Pancreatic tissue integrity is restored in animals treated with PP2 before CER stimulation. Shown are micrographs of H&E histological sections of pancreata from rats treated as described in a and b). Sections from control pancreas (c) showed a normal acinar organization and staining, whereas CER treatment (d) induced large edematous voids, vacuolization, and cell damage. In contrast, tissue from rats treated with PP2 before CER administration (e) showed a morphology remarkably similar to that of control animals.

ACKNOWLEDGMENTS

We thank Heather M. Thompson (Mayo Clinic) for help in preparing the manuscript.

REFERENCES

Adler, G., Kern, H. F., Pan, G. Z., and Gardner, J. D. (1984). Secretagogue-induced membrane alterations in dispersed acini from rat pancreas. Eur. J. Cell Biol. *33*, 234–241.

Anderson, R. D., Haskell, R. E., Xia, H., Roessler, B. J., and Davidson, B. L. (2000). A simple method for the rapid generation of recombitant adenovirus vectors. Gene Ther. *7*, 1034–1038.

Bhatia, M., Wong, F. L., Cao, Y., Lau, H. Y., Huang, J., Puneet, P., and Chevali, L. (2005). Pathophysiology of acute pancreatitis. Pancreatology *5*, 132–144.

Burnham, D. B., Soling, H. D., and Williams, J. A. (1988). Evaluation of myosin light chain phosphorylation in isolated pancreatic acini. Am. J. Physiol. *254*, G130–G134.

Burnham, D. B., and Williams, J. A. (1982). Effects of high concentrations of secretagogues on the morphology and secretory activity of the pancreas: a role for microfilaments. Cell Tissue Res. *222*, 201–212.

Cao, H., Orth, J. D., Chen, J., Weller, S. G., Heuser, J. E., and McNiven, M. A. (2003). Cortactin is a component of clathrin-coated pits and participates in receptor-mediated endocytosis. Mol. Cell Biol. *23*, 2162–2170.

Daly, R. J. (2004). Cortactin signalling and dynamic actin networks. Biochem. J. *382*, 13–25.

Dudek, S. M., Jacobson, J. R., Chiang, E. T., Birukov, K. G., Wang, P., Zhan, X., and Garcia, J. G. (2004). Pulmonary endothelial cell barrier enhancement by sphingosine 1-phosphate: roles for cortactin and myosin light chain kinase. J. Biol. Chem. *279*, 24692–24700.

Fallon, M. B., Gorelick, F. S., Anderson, J. M., Mennone, A., Saluja, A., and Steer, M. L. (1995). Effect of cerulein hyperstimulation on the paracellular barrier of rat exocrine pancreas. Gastroenterology *108*, 1863–1872.

Garcia, J. G., Verin, A. D., Schaphorst, K., Siddiqui, R., Patterson, C. E., Csortos, C., and Natarajan, V. (1999). Regulation of endothelial cell myosin light chain kinase by Rho, cortactin, and p60(src). Am. J. Physiol. *276*, L989–L998.

Gourlay, C. W., and Ayscough, K. R. (2005). The actin cytoskeleton: a key regulator of apoptosis and ageing? Nat. Rev. Mol. Cell Biol. *6*, 583–589.

Huang, C., Liu, J., Haudenschild, C. C., and Zhan, X. (1998). The role of tyrosine phosphorylation of cortactin in the locomotion of endothelial cells. J. Biol. Chem. *273*, 25770–25776.

Husain, S. Z., Prasad, P., Grant, W. M., Kolodecik, T. R., Nathanson, M. H., and Gorelick, F. S. (2005). The ryanodine receptor mediates early zymogen activation in pancreatitis. Proc. Natl. Acad. Sci. USA *102*, 14386–14391.

Jungermann, J., Lerch, M. M., Weidenbach, H., Lutz, M. P., Kruger, B., and Adler, G. (1995). Disassembly of rat pancreatic acinar cell cytoskeleton during supramaximal secretagogue stimulation. Am. J. Physiol. *268*, G328–G338.

Lampel, M., and Kern, H. F. (1977). Acute interstitial pancreatitis in the rat induced by excessive doses of a pancreatic secretagogue. Virchows Arch. A Pathol. Anat. Histol. *373*, 97–117.

Leser, J., Beil, M. F., Musa, O. A., Adler, G., and Lutz, M. P. (2000). Regulation of adherens junction protein p120(ctn) by 10 nM CCK precedes actin breakdown in rat pancreatic acini. Am. J. Physiol. Gastrointest. Liver Physiol. *278*, G486–G491.

Lua, B. L., and Low, B. C. (2005). Cortactin phosphorylation as a switch for actin cytoskeletal network and cell dynamics control. FEBS Lett. *579*, 577–585.

Lynch, G., Kohler, S., Leser, J., Beil, M., Garcia-Marin, L. J., and Lutz, M. P. (2004). The tyrosine kinase Yes regulates actin structure and secretion during pancreatic acinar cell damage in rats. Pflugers Arch. *447*, 445–451.

Muallem, S., Kwiatkowska, K., Xu, X., and Yin, H. L. (1995). Actin filament disassembly is a sufficient final trigger for exocytosis in nonexcitable cells. J. Cell Biol. *128*, 589–598.

Nozu, F., Owyang, C., and Tsunoda, Y. (2000). Involvement of phosphoinositide 3-kinase and its association with pp60src in cholecystokinin-stimulated pancreatic acinar cells. Eur. J. Cell Biol. *79*, 803–809.

O'Konski, M. S., and Pandol, S. J. (1990). Effects of caerulein on the apical cytoskeleton of the pancreatic acinar cell. J. Clin. Invest. *86*, 1649–1657.

O'Konski, M. S., and Pandol, S. J. (1993). Cholecystokinin JMV-180 and caerulein effects on the pancreatic acinar cell cytoskeleton. Pancreas *8*, 638–646.

Pace, A., Tapia, J. A., Garcia-Marin, L. J., and Jensen, R. T. (2006). The Src family kinase, Lyn, is activated in pancreatic acinar cells by gastrointestinal hormones/neurotransmitters and growth factors which stimulate its association with numerous other signaling molecules. Biochim. Biophys. Acta *1763*, 356–365.

Paluch, E., Sykes, C., Prost, J., and Bornens, M. (2006). Dynamic modes of the cortical actomyosin gel during cell locomotion and division. Trends Cell Biol. *16*, 5–10.

Pandol, S. J., Saluja, A. K., Imrie, C. W., and Banks, P. A. (2007). Acute pancreatitis: bench to the bedside. Gastroenterology *132*, 1127–1151.

Saito, I., Hashimoto, S., Saluja, A., Steer, M. L., and Meldolesi, J. (1987). Intracellular transport of pancreatic zymogens during caerulein supramaximal stimulation. Am. J. Physiol. *253*, G517–G526.

Scheele, G., Adler, G., and Kern, H. (1987). Exocytosis occurs at the lateral plasma membrane of the pancreatic acinar cell during supramaximal secretagogue stimulation. Gastroenterology *92*, 345–353.

Torgerson, R. R., and McNiven, M. A. (1998). The actin-myosin cytoskeleton mediates reversible agonist-induced membrane blebbing. J. Cell Sci. *111*, 2911–2922.

Watanabe, O., Baccino, F. M., Steer, M. L., and Meldolesi, J. (1984). Supramaximal caerulein stimulation and ultrastructure of rat pancreatic acinar cell: early morphological changes during development of experimental pancreatitis. Am. J. Physiol. *246*, G457–G467.

Waterford, S. D., Kolodecik, T. R., Thrower, E. C., and Gorelick, F. S. (2005). Vacuolar ATPase regulates zymogen activation in pancreatic acini. J. Biol. Chem. *280*, 5430–5434.

Weaver, A. M., Young, M. E., Lee, W. L., and Cooper, J. A. (2003). Integration of signals to the Arp2/3 complex. Curr. Opin. Cell Biol. *15*, 23–30.

Weed, S. A., and Parsons, J. T. (2001). Cortactin: coupling membrane dynamics to cortical actin assembly. Oncogene *20*, 6418–6434.